Modification of Born impurity scattering near the surface of *d*-wave superconductors and influence of external magnetic field

A. Zare, A. Markowsky, T. Dahm, and N. Schopohl
Institut für Theoretische Physik and Center for Collective Quantum Phenomena, Universität Tübingen, Auf der Morgenstelle 14, D-72076 Tübingen, Germany

(Received 28 July 2008; revised manuscript received 9 September 2008; published 25 September 2008)

We study the influence of self-consistent Born impurity scattering on the zero-energy Andreev bound states near the surface of a *d*-wave superconductor with and without an externally applied magnetic field. Without an external magnetic field we show that the effect of Born impurity scattering is stronger at the surface than in the bulk. In the presence of an external magnetic field the splitting of the zero-energy Andreev bound states is shown to have a nonmonotonous temperature dependence. Born impurity scattering does not wash out the peak splitting, but instead the peak splitting is shown to be quite robust against impurities. We also show that a nonzero renormalization of the pair potential appears near the surface.

DOI: 10.1103/PhysRevB.78.104524 PACS number(s): 74.20.Rp, 74.45.+c, 74.62.Dh

I. INTRODUCTION

At the surface of *d*-wave superconductors zero-energy Andreev bound states may appear depending on the orientation of the *d*-wave with respect to the surface normal.[1–4] Experimentally, these states can be observed as zero-bias conductance peaks in the tunneling conductance.[5–8] It is well known that surface roughness, surface disorder,[9] or diffuse scattering at the surface leads to a broadening of these states. Also, impurity scattering in the bulk of the superconductor is known to broaden the Andreev bound states.[10,11] In the presence of an external magnetic field the screening current leads to a splitting of the Andreev bound states.[12–14] In this case, a counter-flowing paramagnetic current is generated by the surface states, which increases with decreasing temperature and may even lead to a reversal of the current flow at the surface resulting in an anomalous Meissner effect.[12,15] This effect has recently been shown to have a strong influence on the Bean-Livingston surface barrier for entrance of vortices into the superconductor.[16]

In the present work we investigate the influence of bulk impurity scattering on the broadening of the surface Andreev bound states and the splitting in an external magnetic field. It has been shown previously that impurity scattering in the Born limit is much more effective in broadening the Andreev bound states than impurity scattering in the unitarity limit.[10,11] In the high-T_c cuprate compounds it is believed that scatterers within the CuO_2 planes act as unitary scatterers and thus should have little influence on the Andreev bound states. However, it has been recognized recently that scatterers sitting between the CuO_2 planes are poorly screened and act as Born scatterers.[17–19] These impurities are thus expected to have a dominating influence on the broadening of the Andreev bound states. For these reasons in the present work we will focus on the influence of impurity scattering in the self-consistent Born approximation. We will show that in this case impurity scattering around zero energy is significantly increased near the surface as compared to the bulk, leading to a larger broadening of the Andreev bound states than expected from the scattering rate in the bulk. The situation changes completely in the presence of an external magnetic field, however. The splitting of the Andreev bound states turns out to be quite robust against Born impurity scattering.

In the bulk of a *d*-wave superconductor the renormalization of the pair potential due to impurity scattering is known to disappear. However, this is not generally the case near a surface because of broken translational symmetry. Here, we will show that a nonzero renormalization of the pair potential appears near the surface unless the orientation of the surface is highly symmetric with respect to the orientation of the *d* wave. Also, in the presence of an external magnetic field the renormalization of the pair potential becomes nonzero.

In Sec. II we will describe our numerical approach. In Sec. III we will first study impurity scattering near a surface of a *d*-wave superconductor in the absence of an external magnetic field. Section IV presents results for a superconductor without impurities in the presence of an external magnetic field, and Sec. V deals with both impurity scattering and the presence of an external magnetic field.

II. NUMERICAL APPROACH

The geometry under investigation is shown in Fig. 1; in the half space $x>0$, we assume to have a superconducting area of *d*-wave type. For $x<0$, an external magnetic field $\vec{B}=B\vec{e}_z$ is applied parallel to the z axis. For simplicity, we consider a cylindrical Fermi surface with the c-axis oriented parallel to the z axis. Also, we assume that the external magnetic field remains smaller than the field of first vortex penetration. Therefore, we can assume translational invariance both along the y axis as well as along the z direction. The relation between the current density in the superconductor and the vector potential in Coulomb gauge is given by Maxwell's equation:

$$-\Delta\vec{A}=\frac{4\pi}{c}\vec{j}. \tag{1}$$

In this gauge the vector potential is directly proportional to the superfluid velocity v_s. The boundary conditions for this second-order differential equation are determined by the be-

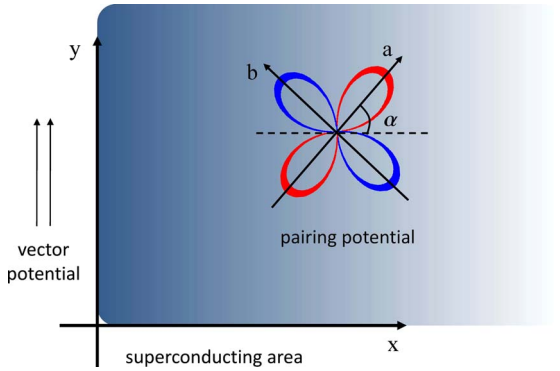

FIG. 1. (Color online) Sketch of the investigated geometry, showing the pair potential and the direction of the vector potential relative to the surface of the superconductor. The angle α determines the relative orientation of the d wave with respect to the surface normal.

havior of the magnetic field; it penetrates into the superconductor continuously and decays to zero in the bulk.

Our calculations are based on the Eilenberger equations.[20,21] These equations can be transformed into Riccati-type differential equations for two scalar complex quantities $a(s)$ and $b(s)$ along real space trajectories $\vec{R}(s)=\vec{r}+s\hat{v}_F$ (Ref. 22):

$$\hbar v_F \frac{\partial}{\partial s} a(s) + [2\tilde{\epsilon}_n(s) + \tilde{\Delta}^\dagger(s) a(s)] a(s) - \tilde{\Delta}(s) = 0$$

$$\hbar v_F \frac{\partial}{\partial s} b(s) - [2\tilde{\epsilon}_n(s) + \tilde{\Delta}(s) b(s)] b(s) + \tilde{\Delta}^\dagger(s) = 0. \quad (2)$$

Here, v_F is the Fermi velocity and $\hat{v}_F$ the unit vector in the direction of the Fermi velocity. The initial values for solving the Riccati equations for $a(s)$ and $b(s)$ are obtained from the fact, that their variation vanishes in the bulk:

$$a(-\infty) = \frac{\tilde{\Delta}(-\infty)}{\tilde{\epsilon}_n + \sqrt{\tilde{\epsilon}_n^2 + |\tilde{\Delta}(-\infty)|^2}} \quad (3)$$

$$b(+\infty) = \frac{\tilde{\Delta}^\dagger(+\infty)}{\tilde{\epsilon}_n + \sqrt{\tilde{\epsilon}_n^2 + |\tilde{\Delta}(+\infty)|^2}}. \quad (4)$$

Here, the renormalized Matsubara energies and pair potential are given by:

$$i\tilde{\varepsilon}_n[\vec{R}(s), \varepsilon_n, T] = i\varepsilon_n + \frac{e}{c}\vec{v}_F \cdot \vec{A}[\vec{R}(s)] - \Sigma^G[\vec{R}(s), \varepsilon_n, T]$$

$$\tilde{\Delta}[\vec{R}(s), \varepsilon_n, T] = \Delta[\vec{R}(s), T]\cos[2(\theta-\alpha)] + \Sigma^F[\vec{R}(s), \varepsilon_n, T],$$

where Σ^G and Σ^F denote the diagonal and off-diagonal self-energies due to impurity scattering. The pair potential is given by:

$$\Delta(\vec{r}, T) = VN_0\pi T \sum_{|\epsilon_n|<\omega_c} \langle \cos[2(\theta-\alpha)] f(\vec{r}, \vec{k}_F, i\epsilon_n)\rangle_{FS}. \quad (5)$$

The brackets $\langle\cdots\rangle_{FS}$ denote an angular average over the cylindrical Fermi surface. By solving the Riccati equations along real space trajectories $\vec{R}(s)$ running parallel to the Fermi velocity $\vec{v}_F$, the normal and anomalous propagators are found from:

$$g[\vec{R}(s)] = (-i)\cdot \frac{1-a(s)b(s)}{1+a(s)b(s)}, \quad f[\vec{R}(s)] = \frac{2a(s)}{1+a(s)b(s)}. \quad (6)$$

From the propagators, we can instantly derive the current density $\vec{j}(\vec{r})$ and the local density of states (LDOS) $N(E,\vec{r})$:

$$\frac{N(E,\vec{r})}{N_0} = -\,\mathrm{Im}\langle g(\vec{r}, \vec{k}_F, i\epsilon_n \to E + i0^+)\rangle_{FS} \quad (7)$$

where N_0 is the normal-state density of states at the Fermi level, and

$$\vec{j}(\vec{r}, T) = 2eN_0 v_F k_B \pi T \sum_{|\epsilon_n|<\omega_c} \langle \hat{v}_F \cdot g(\vec{r}, \vec{k}_F, i\epsilon_n)\rangle_{FS}. \quad (8)$$

The zero-temperature London penetration depth λ_L is given by the expression $\lambda_L^{-2} = \frac{4\pi}{c^2} e^2 N_0 v_F^2$. Throughout the work we will quote λ_L relative to the zero-temperature coherence length without impurities $\xi_0 = \frac{\hbar v_F}{\pi\Delta(T=0)}$, i.e., the parameter $\kappa = \lambda_L/\xi_0$. Magnetic fields will be given in units of the zero-temperature upper critical field B_{c2}, which for a bulk d-wave superconductor is given by $B_{c2} = 0.49\frac{\Phi_0}{2\pi\xi_0^2}$ for a cylindrical Fermi surface.

In our model, we include the effect of impurity scattering in the self-consistent Born approximation. As pointed out above, Born impurity scattering is expected to cause a stronger effect than scattering in the unitarity limit.[10,11] For simplicity, we will restrict ourselves to s-wave scattering. In this case the impurity self-energies are given by:

$$\Sigma^F(\vec{r}, \epsilon_n, T) = \frac{1}{2\tau}\langle f(\vec{r}, \vec{k}_F, \epsilon_n)\rangle_{FS} \quad (9)$$

$$\Sigma^G(\vec{r}, \epsilon_n, T) = \frac{1}{2\tau}\langle g(\vec{r}, \vec{k}_F, \epsilon_n)\rangle_{FS}, \quad (10)$$

where τ is the scattering lifetime in the bulk and is given by:

$$\frac{1}{\tau} = \frac{2}{\hbar}\pi N_0 n_i |V_0|^2,$$

where n_i is the impurity concentration and V_0 is the strength of the impurity potential. Throughout this work, we will quantify the impurity scattering in terms of its mean-free path $l = v_F\tau$ relative to the zero-temperature bulk coherence length in the superclean limit ξ_0. In the bulk of a d-wave superconductor the angular average of the anomalous Green's function f over the Fermi surface vanishes, because positive and negative contributions cancel exactly. This leads to a vanishing renormalization Σ^F of the pair potential. How-

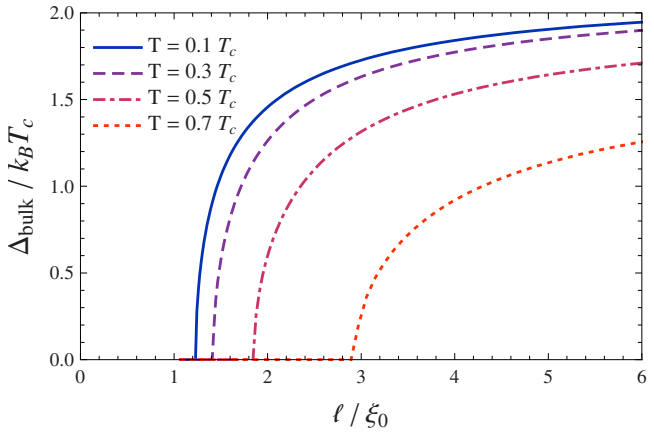

FIG. 2. (Color online) Bulk value of the pair potential as a function of mean-free path l/ξ_0 for different temperatures.

ever, as we will show below, this does not generally hold anymore in the vicinity of a surface.

Numerically, we start with estimated functions $\tilde{\Delta}(x)$ and $\vec{A}(x)$. These are used to solve the Riccati equations [Eq. (2)] along all real space trajectories with specular reflection on the surface $x=0$. From the solutions we find the propagators [Eq. (6)]. These are used to obtain the self-energies [Eqs. (9) and (10)], the current density [Eq. (8)], and the updated pair potential [Eq. (5)]. Finally, integration of Eq. (1) yields an updated vector potential. This procedure is iterated until the functions $\tilde{\Delta}(x)$ and $\vec{A}(x)$ converge. Note that the self-energies Σ^G and Σ^F and the propagators g and f are calculated self-consistently this way. After convergence, a final iteration is run, in which all equations are solved directly for real frequencies $i\epsilon_n \rightarrow E+i0^+$ in order to perform an analytic continuation for the local density of states and the self-energies. Only for the calculations without impurities we have added a small imaginary part of $0.007k_BT_c$ in order to regularize the poles of the propagators.

III. IMPURITY SCATTERING NEAR A SURFACE OF A *d*-WAVE SUPERCONDUCTOR

In this section we consider a superconductor with different impurity concentrations for the case that no external magnetic field is applied. It is well known that impurities in bulk *d*-wave superconductors lead to pair breaking, which implies a decrease of the bulk order parameter. Figure 2 shows the bulk value of the pair potential as a function of the mean-free path l for different temperatures. When the mean-free path becomes comparable to the finite temperature coherence length, the pair potential vanishes. Consequently, for *d*-wave superconductors, there exists no real dirty limit.

Near the surface, Andreev bound states are absent for *d*-wave orientation $\alpha=0$. When the angle α is increased, the spectral weight of the Andreev bound states gradually increases until it reaches a maximum at $\alpha=\pi/4$. In the following we will first focus on an intermediate angle of $\alpha=\pi/8$, where the spectral weight is neither absent nor fully developed.

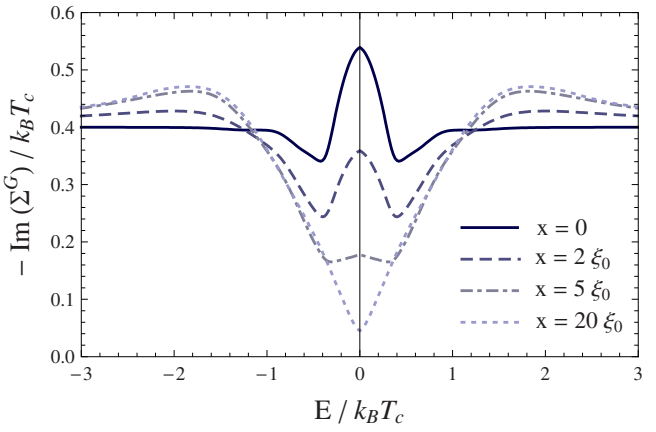

FIG. 3. (Color online) Negative imaginary part of self-energy Σ^G as a function of energy E for different distances from the surface at an orientation angle of $\alpha=\frac{\pi}{8}$. The temperature is $T=0.1T_c$ and the mean-free path $l=2.7\xi_0$.

The local quasiparticle scattering rate is given by the negative imaginary part of the normal self-energy $-\mathrm{Im}\,\Sigma^G$. In Fig. 3 we show the energy dependence of $-\mathrm{Im}\,\Sigma^G$ for different distances from the surface at a temperature $T=0.1T_c$ and a mean-free path of $l=2.7\xi_0$. From this it can be seen that there is a significant variation of the quasiparticle scattering rate at the Fermi level $E=0$ as a function of the distance from the surface. For this set of parameters, at the surface the quasiparticle scattering rate is about 12 times larger than in the bulk. Physically, this effect can be understood from Eq. (10). At the surface in the presence of the Andreev bound states there is a larger phase space of low energy states available for scattering. This makes impurity scattering more effective at the surface than in the bulk.

In Fig. 4, the impurity dependence of the local density of states at the surface is shown for the same angle α and temperature. Increasing the impurity concentration results in a decrease of the height of the zero-energy peak and a broadening of its width. The peaks seen near $1.4k_BT_c$ and $0.9k_BT_c$ in the absence of impurity scattering can be interpreted as follows: the peaks near $\pm 1.4k_BT_c$ are related to the bulk gap

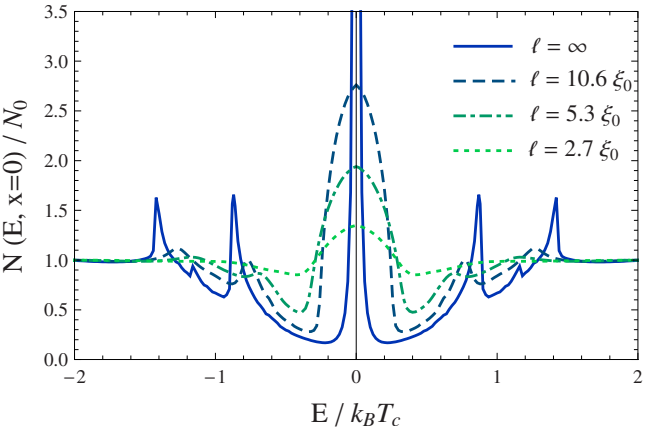

FIG. 4. (Color online) Local density of states at the surface for different impurity concentrations. The temperature is $T=0.1T_c$ and the orientation angle $\alpha=\frac{\pi}{8}$.

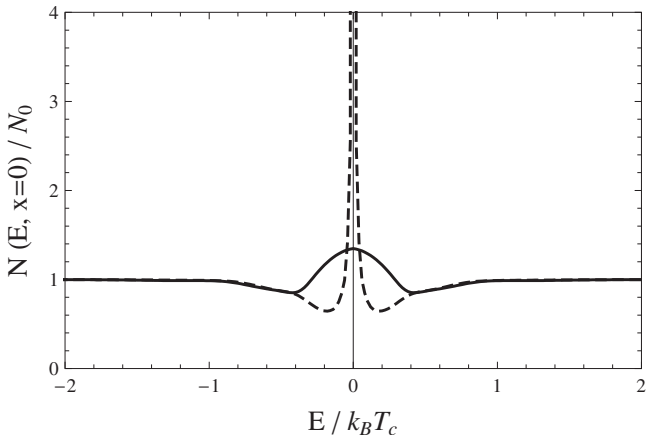

FIG. 5. The local density of states at the surface for temperature $T=0.1T_c$, orientation angle $\alpha=\frac{\pi}{8}$, and mean-free path $l=2.7\xi_0$. The dashed curve shows the LDOS when the bulk values of the self-energy are used. The solid curve, on the other hand, shows the LDOS when using the self-consistent solution for the self-energy.

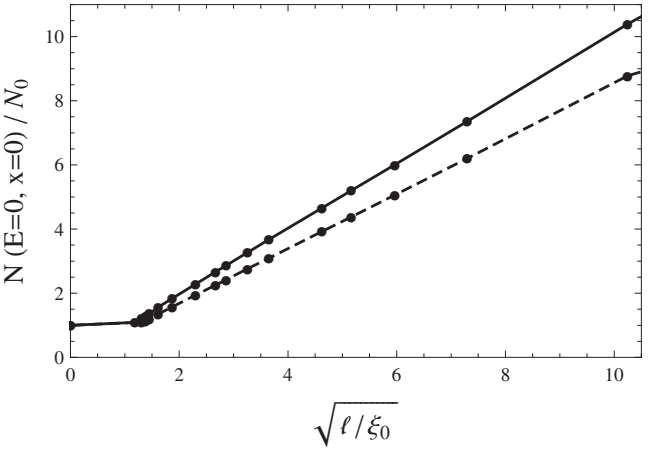

FIG. 6. Zero energy density of states at the surface as a function of $\sqrt{\frac{l}{\xi_0}}$ for two different orientations $\alpha=\frac{\pi}{4}$ (solid) and $\alpha=\frac{\pi}{8}$ (dashed). Temperature is $T=0.1T_c$.

times $\cos 2\alpha$. They are coming from quasiparticles, which approach the surface perpendicular, as a look at the momentum resolved data shows. In contrast, the peaks near $\pm 0.9k_BT_c$ are caused by grazing angle quasiparticles. In our self-consistent calculation the local gap near the surface is much smaller than in the bulk. The grazing angle quasiparticles mostly experience the reduced surface gap value, creating a gap edge around $0.9k_BT_c$. In the presence of impurities these gap features are quickly washed out.

In order to illustrate the change of the local density of states at the surface due to impurity scattering, in Fig. 5 we compare the local density of states at the surface for $l=2.7\xi_0$ with a hypothetical calculation, in which we have used the bulk value of Σ^G at the surface. Clearly, the zero-energy peak is much sharper when the bulk Σ^G is used for the calculation.

These results show that the influence of Born impurity scattering is much stronger at the surface than in the bulk due to the presence of the Andreev bound states. Their presence creates a larger number of available scattering channels, which in turn leads to a stronger broadening of the Andreev bound states. This self-consistent broadening can be illustrated by looking at the peak height of the local density of states at zero energy $N(E=0)/N_0$. On the one hand the peak height scales approximately with the inverse of the local quasiparticle scattering rate:

$$\frac{N(E=0)}{N_0} \sim \frac{k_BT_c}{-\mathrm{Im}\,\Sigma^G(E=0)}.$$

On the other hand the local quasiparticle scattering rate is determined by the peak height via Eq. (10):

$$-\mathrm{Im}\,\Sigma^G(E=0) = \frac{1}{2\tau}\frac{N(E=0)}{N_0}.$$

Solving for the peak height leads to the expression

$$\frac{N(E=0)}{N_0} \sim \sqrt{2\pi k_BT_c} \sim \sqrt{\frac{l}{\xi_0}}.$$

This result is in good agreement with the numerical result shown in Fig. 6. It shows that the scaling behavior of the peak height is $\sim\sqrt{l}$ instead of the $\sim l$ behavior one would have expected from bulk scattering, leading to a stronger impurity effect near the surface.

In an isotropic *s*-wave superconductor Anderson's theorem asserts that the renormalization of the pair potential due to the anomalous self-energy Σ^F exactly compensates the renormalization due to the normal self-energy Σ^G, such that the density of states and T_c remain unaffected by impurity scattering. This does not necessarily hold anymore in an anisotropic superconductor, however.[23] In the bulk of a *d*-wave superconductor the anomalous self-energy Σ^F is known to vanish. This is clear from Eq. (9), because the Fermi surface average leads to cancellation due to the sign change of the *d* wave. Ultimately, this is the reason why nonmagnetic impurity scattering is much more destructive to unconventional superconductors than to conventional ones. It has not been noted before, however, that this vanishing of Σ^F for *d*-wave superconductors is not generally true anymore near the surface. Near the surface, translational invariance is broken, which makes trajectories with different momenta k_F inequivalent, because they experience different pair potential landscapes. Except for special orientations α of the *d* wave with respect to the surface this leads to finite values of the anomalous self-energy Σ^F. In Fig. 7 we show the real part of Σ^F at the surface as a function of the orientation angle α for different energies. It can be seen that Σ^F vanishes for integer multiples of $\pi/4$. Figure 8 shows how Σ^F varies with the distance from the surface and energy (inset) for $\alpha=\pi/8$ decreasing to zero in the bulk.

IV. INFLUENCE OF AN EXTERNAL MAGNETIC FIELD IN THE CLEAN LIMIT

In this section we will discuss the influence of an external magnetic field in the absence of impurity scattering. In par-

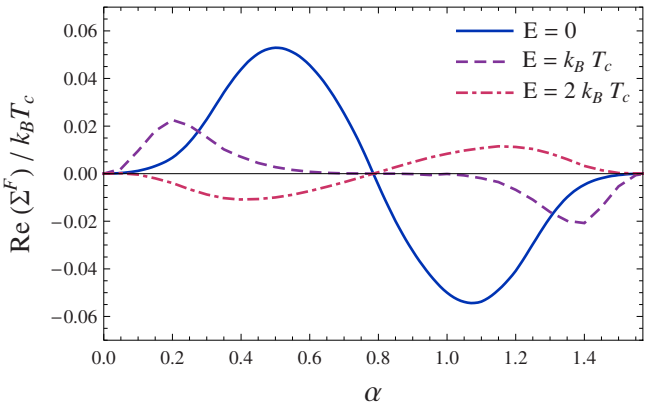

FIG. 7. (Color online) Real part of self-energy Σ^F at the surface vs orientation angle α for different energies. The temperature is $T=0.5T_c$ and the mean-free path $l=2.7\xi_0$.

ticular we focus on the case $\alpha=\frac{\pi}{4}$, where the spectral weight of the Andreev bound states is strongest and $\kappa=10$. This value of κ is modest in comparison with κ values of hole doped high-T_c cuprates, but may be relevant for some low T_c electron doped cuprates.[24] The influence of the anomalous Meissner effect becomes more pronounced for small values of κ and here we wish to illustrate a peculiar effect that occurs in this range of parameters.

In the following we have set the external magnetic field to $B_{\text{ext}}=0.02B_{c2}$. Figure 9 shows the current density for selected temperatures as a function of the distance from the surface. In a distance up to $3\xi_0$ from the surface (which is of the order of the spatial extension of the bound states), the current is flowing opposite to the screening current.[12,15] This anomalous Meissner current persists throughout the full temperature range between $0.01T_c$ and $0.9T_c$, as demonstrated in the inset of Fig. 9. While it is nearly vanishing for temperatures close to T_c, it saturates near zero temperature.

The magnetic field distributions resulting from the current distributions are shown in Fig. 10. With the anomalous

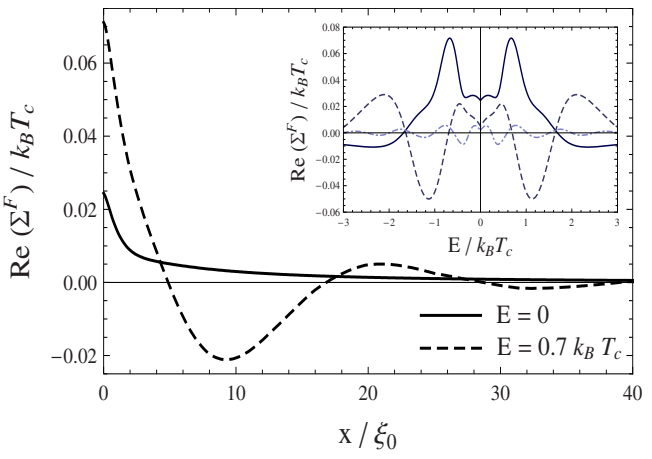

FIG. 8. (Color online) Real part of the self-energy Σ^F vs distance for two different energies E. The inset shows the energy dependence of this self-energy for different distances from the surface: $x/\xi_0=0$ (solid line), $x/\xi_0=5$ (dashed line), and $x/\xi_0=20$ (dashed-dotted line). In both cases, the orientation is given by $\alpha=\frac{\pi}{8}$, the mean-free path $l=2.7\xi_0$, and the temperature is $T=0.1T_c$.

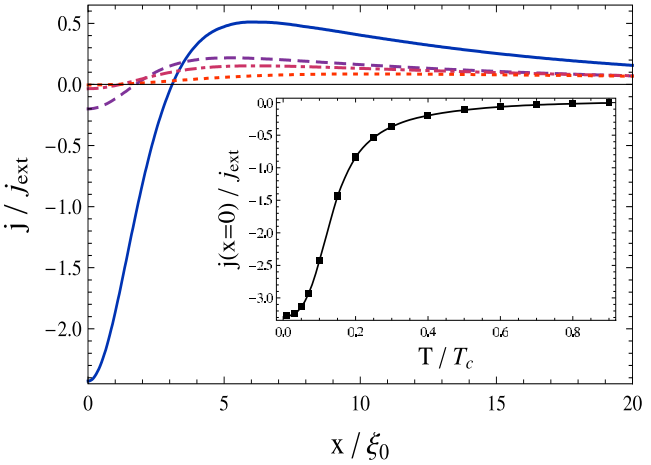

FIG. 9. (Color online) Current density distribution for orientation $\alpha=\frac{\pi}{4}$ at temperatures $T=0.1T_c$ (solid), $0.4T_c$ (dashed), $0.7T_c$ (dashed-dotted), $0.9T_c$ (dotted). The external magnetic field is $B_{\text{ext}}=0.02B_{c2}$. The inset shows the temperature dependence of the surface current density for orientation $\alpha=\frac{\pi}{4}$ and the same value of the external magnetic field. Here, the current density has been normalized to $j_{\text{ext}}=\frac{c}{4\pi}\frac{B_{\text{ext}}}{\lambda_L}$.

Meissner current flowing, the magnetic field initially increases before the normal Meissner screening sets in and eventually screens out the magnetic field exponentially. This initial increase occurs again up to a distance of $\sim 3\xi_0$ from the surface. With the value of $\kappa=10$ we have used here, the field increases by more than a factor of 2 relative to the external field. Qualitatively it is clear that this field increase becomes more pronounced for smaller values of κ, because a smaller penetration depth results in larger current densities, as seen from Eq. (8).

Figure 11 shows the modulus of the vector potential at the surface as a function of temperature. It can be seen that the temperature dependence is nonmonotonous. The vector potential increases both toward low temperatures as well as toward T_c. The behavior near T_c is easily understood from the temperature dependence of the penetration depth, which diverges near T_c. Since the vector potential is the integral of

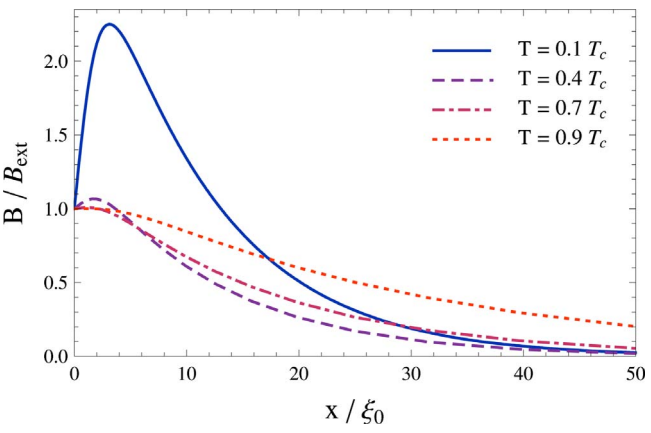

FIG. 10. (Color online) Magnetic field as a function of the distance from the surface for orientation $\alpha=\frac{\pi}{4}$ and different temperatures. The external magnetic field is $B_{\text{ext}}=0.02B_{c2}$.

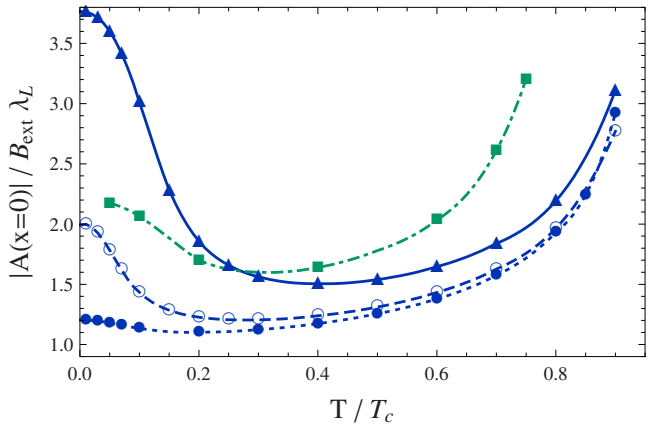

FIG. 11. (Color online) Temperature dependence of the surface vector potential for orientation $\alpha=\frac{\pi}{4}$. Results are shown for $\kappa=10$ and $B_{\text{ext}}=0.02B_{c2}$ (triangles), $\kappa=30$ and $B_{\text{ext}}=0.006B_{c2}$ (open circles), $\kappa=63$ and $B_{\text{ext}}=0.006B_{c2}$ (filled circles). For comparison, the squares show the result for $\kappa=10$ and $B_{\text{ext}}=0.02B_{c2}$ including impurity scattering with a mean-free path of $l=5.3\xi_0$. Lines are guide to the eye.

the magnetic field, at a fixed external magnetic field we have to expect an increasing vector potential with increasing penetration depth. The increase of the surface vector potential toward low temperatures has a different physical origin; it is directly related to the anomalous Meissner effect and the field increase shown in Fig. 10.

Since the vector potential is proportional to the superfluid velocity, this nonmonotonous temperature dependence of the vector potential has a direct influence on the size of the peak splitting in the local density of states,[12] which we show in Fig. 12. It can be seen that the splitting is large both for low temperatures and close to T_c. As a result also the peak height has a nonmonotonous temperature dependence. The observation of such an increase of the peak splitting toward low temperatures could be an experimental signature of the anomalous Meissner currents. It should be pointed out, however, that this effect becomes less pronounced the larger the κ value of the material. This is shown in Fig. 11 for $\kappa=30$ and $\kappa=63$ as the open and solid circles, respectively. For these higher values of κ the increase of the vector potential toward low temperatures is gradually reduced. We also want to mention that impurity scattering gradually reduces this low temperature increase. The squares in Fig. 11 show the behavior for $\kappa=10$ and a mean-free path of $l=5.3\xi_0$. The low temperature increase is reduced, while the increase toward T_c is shifted due to the reduction of the bulk T_c.

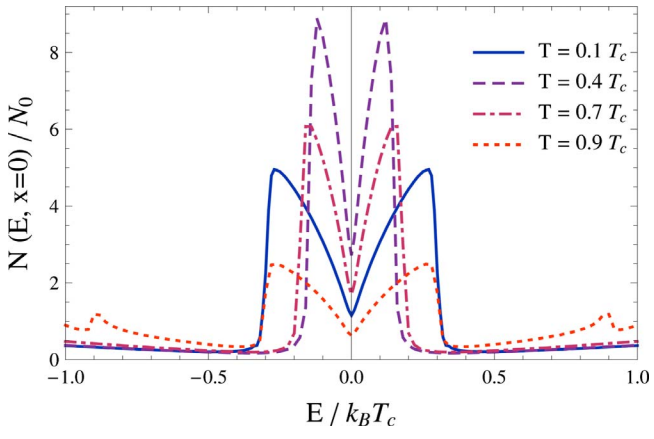

FIG. 12. (Color online) Nonmonotonous splitting of the local density of states for orientation $\alpha=\frac{\pi}{4}$ at different temperatures. The magnetic field is $B=0.02B_{c2}$.

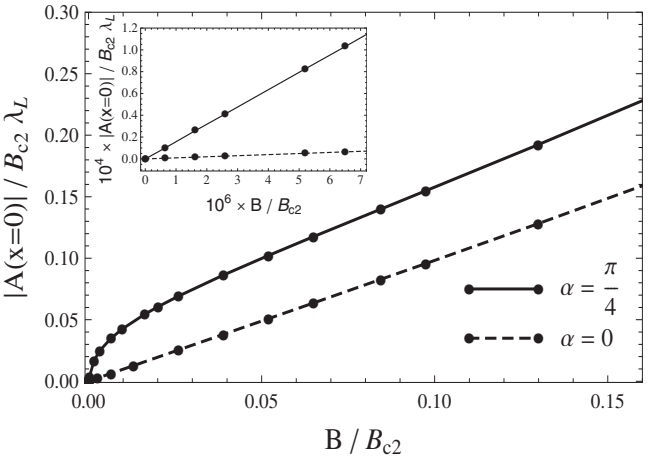

FIG. 13. Surface vector potential as a function of the external magnetic field B/B_{c2} for temperature $T=0.1T_c$ and $\kappa=10$. The solid line shows the result for $\alpha=\frac{\pi}{4}$ and the dashed line for $\alpha=0$. In the inset the low-field range is shown.

The presence of the surface Andreev bound states also has a significant influence on the nonlinear Meissner effect. We demonstrate this in Fig. 13, which shows the surface vector potential as a function of the external magnetic field for orientations $\alpha=\frac{\pi}{4}$ (solid line) and $\alpha=0$ (dashed line). For $\alpha=0$, where surface Andreev bound states are absent, the response is linear over a broad range of magnetic fields. In contrast, for $\alpha=\frac{\pi}{4}$ sizeable nonlinear corrections are visible, seen as a steep increase at low fields. In the low-field range of the order of $\sim 10^{-5}B_{c2}$, shown in the inset, the response is linear in both cases with a significantly larger slope at $\alpha=\frac{\pi}{4}$. We suppose that this surface related effect may have an important influence on the nonlinear Meissner effect in d-wave superconductors and intermodulation distortion generated in high-T_c microwave resonators.[25–27]

V. INFLUENCE OF IMPURITY SCATTERING ON THE PEAK SPLITTING

Having discussed the two limiting cases of impurity scattering without an external magnetic field and the influence of a magnetic field without impurity scattering, we turn now to a discussion of the combined effect of impurity scattering in the presence of an external magnetic field. Naively, one might expect that the impurity scattering will wash out the peak splitting. We will show below that the situation is more complex, however. In the following we will work with a value of $\kappa=63$, which is more realistic for hole doped high-T_c cuprates.

In Fig. 14 we demonstrate the influence of impurity scattering on the peak splitting of the local density of states at

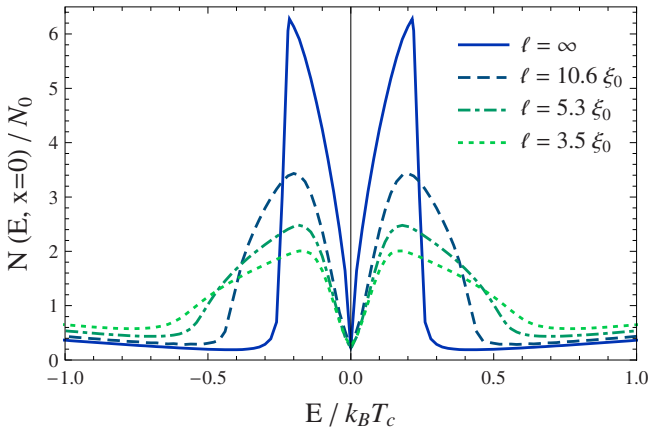

FIG. 14. (Color online) Local density of states at the surface for different impurity mean-free paths in the presence of an external magnetic field $B=0.006B_{c2}$. The temperature is $T=0.1T_c$ and the orientation angle $\alpha=\frac{\pi}{4}$.

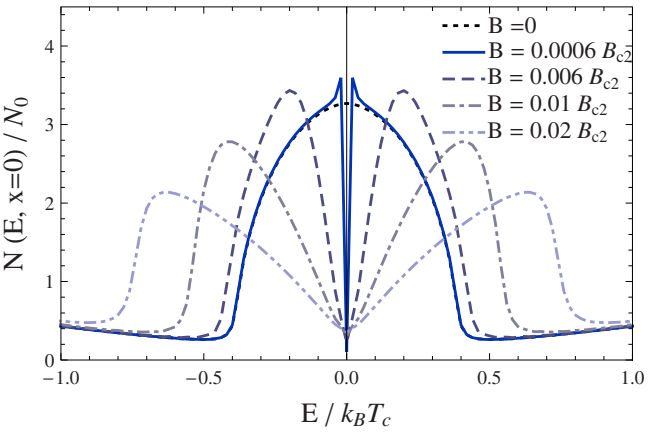

FIG. 16. (Color online) Local density of states at the surface for different external magnetic fields with mean-free path $l=10.6\xi_0$. The temperature is $T=0.1T_c$ and the orientation angle $\alpha=\frac{\pi}{4}$.

the surface. Here we have chosen a surface angle $\alpha=\frac{\pi}{4}$, temperature $T=0.1T_c$, and an external magnetic field of $B=0.006B_{c2}$. It can be seen that the peak height is strongly reduced and the peak width grows with decreasing mean-free path. However, the size of the peak splitting remains almost unaffected. This peculiar effect can be understood from the energy dependence of the negative imaginary part of the self-energy Σ^G, which is shown in Fig. 15. Here we can see that the scattering rate also shows a splitting in energy, which is just the mirror image of the splitting in the local density of states. It results from the fact that due to the peak splitting the available phase space for scattering processes is strongly reduced at low energies. This in turn means that the quasiparticle scattering rate at small energies remains small even when the mean-free path becomes small. This leads to a self-stabilization of the peak splitting making it robust against impurity scattering.

In Fig. 16 we show the peak splitting for a fixed mean-free path $l=10.6\xi_0$ and a series of external magnetic fields. When the magnetic field is increased, the peak splitting does not evolve as a dip near zero energy, which gradually becomes deeper, but instead the splitting opens up like a curtain. Note that the frequency dependence at low energy is approximately linear over an increasing energy scale and the two peaks get a triangular lineshape.

In the absence of an external magnetic field we have pointed out above that the anomalous self-energy Σ^F does not vanish except for certain highly symmetric angles such as $\alpha=\pi/4$. In the presence of an external magnetic field even for $\alpha=\pi/4$, the anomalous self-energy Σ^F does not vanish anymore. This is shown in Fig. 17, where the imaginary part of Σ^F is shown as a function of energy for different distances from the surface. The reason for this is that the special reflection symmetry of the case $\alpha=\pi/4$ is broken now by the direction of the current flow.

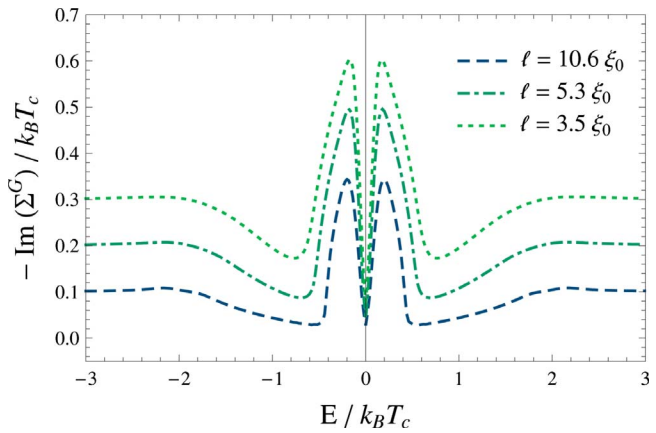

FIG. 15. (Color online) Negative imaginary part of the self-energy Σ^G at the surface for different impurity concentrations in the presence of an external magnetic field $B=0.006B_{c2}$. The temperature is $T=0.1T_c$ and the orientation angle $\alpha=\frac{\pi}{4}$.

VI. CONCLUSIONS

We have studied the influence of self-consistent Born impurity scattering on the surface Andreev bound states in a d-wave superconductor. In the absence of an external

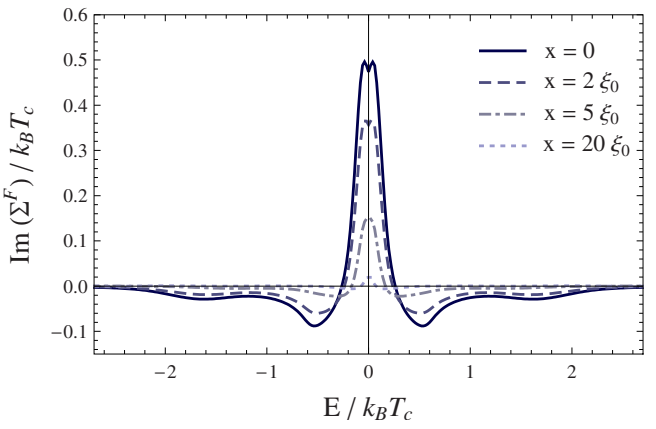

FIG. 17. (Color online) Imaginary part of the off-diagonal self-energy with external magnetic field $B=0.006B_{c2}$ for orientation $\alpha=\frac{\pi}{4}$, temperature $T=0.1T_c$ and $l=3.5\xi_0$.

magnetic-field Born impurity scattering leads to a broadening of the zero-energy peak in agreement with previous work.[10,11] We have shown, however, that the effect of the impurities is much stronger at the surface than in the bulk. Also, the renormalization of the pair potential in general does not vanish anymore near the surface.

In the presence of an external magnetic field we have demonstrated that for small values of $\kappa \sim 10$ the zero-energy peak splitting has a strongly nonmonotonous temperature dependence. For fixed external magnetic field the peak splitting is larger at small and at high temperatures and has a minimum in the intermediate temperature range. We have also shown that the presence of Andreev bound states leads to significant nonlinear corrections to the Meissner effect. The range of κ values in question is small compared with hole doped high-T_c cuprate materials. However, we suggest that these effects may be observable in some electron-doped cuprates, which have smaller κ values due to a lower T_c and larger carrier densities.[24]

We have shown further that the peak splitting turns out to be quite robust against Born impurity scattering. This results from a self-stabilizing effect of the peak splitting.

ACKNOWLEDGMENTS

This work was supported by the Deutsche Forschungsgemeinschaft through project No. DA 514/2-1. We thank S. Graser and C. Iniotakis for valuable discussions.

[1] C. R. Hu, Phys. Rev. Lett. **72**, 1526 (1994).
[2] Y. Tanaka and S. Kashiwaya, Phys. Rev. Lett. **74**, 3451 (1995).
[3] L. J. Buchholtz, M. Palumbo, D. Rainer, and J. A. Sauls, J. Low Temp. Phys. **101**, 1099 (1995).
[4] S. Kashiwaya and Y. Tanaka, Rep. Prog. Phys. **63**, 1641 (2000).
[5] M. Covington, M. Aprili, E. Paraoanu, L. H. Greene, F. Xu, J. Zhu, and C. A. Mirkin, Phys. Rev. Lett. **79**, 277 (1997).
[6] B. Chesca, M. Seifried, T. Dahm, N. Schopohl, D. Koelle, R. Kleiner, and A. Tsukada, Phys. Rev. B **71**, 104504 (2005).
[7] G. Deutscher, Rev. Mod. Phys. **77**, 109 (2005).
[8] M. Wagenknecht, D. Koelle, R. Kleiner, S. Graser, N. Schopohl, B. Chesca, A. Tsukada, S. T. B. Goennenwein, and R. Gross, Phys. Rev. Lett. **100**, 227001 (2008), and references therein.
[9] M. S. Kalenkov, M. Fogelström, and Yu. S. Barash, Phys. Rev. B **70**, 184505 (2004).
[10] A. Poenicke, Yu. S. Barash, C. Bruder, and V. Istyukov, Phys. Rev. B **59**, 7102 (1999); Yu. S. Barash, M. S. Kalenkov, and J. Kurkijärvi, *ibid.* **62**, 6665 (2000).
[11] Y. Tanaka, Y. Tanuma, and S. Kashiwaya, Phys. Rev. B **64**, 054510 (2001).
[12] M. Fogelström, D. Rainer, and J. A. Sauls, Phys. Rev. Lett. **79**, 281 (1997).
[13] M. Aprili, E. Badica, and L. H. Greene, Phys. Rev. Lett. **83**, 4630 (1999).
[14] R. Krupke and G. Deutscher, Phys. Rev. Lett. **83**, 4634 (1999).
[15] H. Walter, W. Prusseit, R. Semerad, H. Kinder, W. Assmann, H. Huber, H. Burkhardt, D. Rainer, and J. A. Sauls, Phys. Rev. Lett. **80**, 3598 (1998).
[16] C. Iniotakis, T. Dahm, and N. Schopohl, Phys. Rev. Lett. **100**, 037002 (2008).
[17] E. Abrahams and C. M. Varma, Proc. Natl. Acad. Sci. U.S.A. **97**, 5714 (2000).
[18] L.-Y. Zhu, P. J. Hirschfeld, and D. J. Scalapino, Phys. Rev. B **70**, 214503 (2004).
[19] T. Dahm, P. J. Hirschfeld, D. J. Scalapino, and L.-Y. Zhu, Phys. Rev. B **72**, 214512 (2005).
[20] G. Eilenberger, Z. Phys. **214**, 195 (1968).
[21] A. I. Larkin and Yu. N. Ovchinnikov, Zh. Eksp. Teor. Fiz. **55**, 2262 (1968) [Sov. Phys. JETP **28**, 1200 (1969)].
[22] N. Schopohl and K. Maki, Phys. Rev. B **52**, 490 (1995); N. Schopohl, arXiv:cond-mat/9804064 (unpublished).
[23] N. Schopohl and K. Scharnberg, Solid State Commun. **22**, 371 (1977), and references therein.
[24] L. Fabrega, B. Martinez, J. Fontcuberta, X. Obradors, and S. Pinol, Phys. Rev. B **46**, 5581 (1992).
[25] S.-K. Yip and J. A. Sauls, Phys. Rev. Lett. **69**, 2264 (1992).
[26] T. Dahm, D. J. Scalapino, and B. A. Willemsen, J. Appl. Phys. **86**, 4055 (1999); T. Dahm and D. J. Scalapino, *ibid.* **81**, 2002 (1997).
[27] D. E. Oates, S.-H. Park, and G. Koren, Phys. Rev. Lett. **93**, 197001 (2004).